Clim. Past Discuss., 9, 3103–3123, 2013
www.clim-past-discuss.net/9/3103/2013/
doi:10.5194/cpd-9-3103-2013

Climate of the Past Discussions
Open Access

On the low frequency component of the ENSO-Indian Monsoon relationship; a paired proxy perspective

M. Berkelhammer[1,2], A. Sinha[3], M. Mudelsee[4,5], H. Cheng[6,7], K. Yoshimura[8], and J. Biswas[9]

[1]University of Colorado, Boulder, USA
[2]Cooperative Institute for Research in Environmental Sciences, Boulder, Colorado, USA
[3]California State University, Dominguez Hills, USA
[4]Climate Risk Analysis, Hanover, Germany
[5]Alfred Wegener Institute, Bremerhaven, Germany
[6]University of Minnesota, Minneapolis, USA
[7]Institute for Global Environmental Change, Xian Jiatong, China
[8]Atmospheric and Oceanic Research Institute, Tokyo, Japan
[9]National Cave Research and Protection Organization, Raipur, India

Received: 1 May 2013 – Accepted: 8 May 2013 – Published: 11 June 2013

Correspondence to: M. Berkelhammer (max.berkelhammer@colorado.edu)

Published by Copernicus Publications on behalf of the European Geosciences Union.

Abstract

There are a number of clear examples in the instrumental period where positive El Niño events were coincident with a severely weakened summer monsoon over India (ISM). ENSO's influence on the Indian Monsoon has therefore remained the centerpiece of various predictive schemes of ISM rainfall for over a century. The teleconnection between the monsoon and ENSO has undergone a protracted weakening since the late 1980's suggesting the strength of ENSO's influence on the monsoon may vary considerably on multidecadal timescales. The recent weakening has specifically prompted questions as to whether this shift represents a natural mode of climate variability or a fundamental change in ENSO and/or ISM dynamics due to anthropogenic warming. The brevity of empirical observations and large systematic errors in the representation of these two systems in state-of-the-art general circulation models hamper efforts to reliably assess the low frequency nature of this dynamical coupling under varying climate forcings. Here we place the 20th century ENSO-Monsoon relationship in a millennial context by assessing the phase angle between the two systems across the time spectrum using a continuous tree-ring ENSO reconstruction from North America and a speleothem oxygen isotope (δ^{18}O) based reconstruction of the ISM. The results suggest that in the high-frequency domain (≤ 15 yr), El Niño (La Niña) events persistently lead to a weakened (strengthened) monsoon consistent with the observed relationship between the two systems during the instrumental period. However, in the low frequency domain (≥ 60 yr), periods of strong monsoon are, in general, coincident with periods of enhanced ENSO variance. This relationship is opposite to which would be predicted dynamically and leads us to conclude that ENSO is not pacing the prominent multidecadal variability that has characterized the ISM over the last millennium.

CPD
9, 3103–3123, 2013

1 Introduction

An improved understanding of the dynamical relationship between the El Niño/Southern Oscillation (ENSO) and the Indian Summer Monsoon (ISM), arguably the two largest sources of interannual climate variability on Earth, has profound societal and scientific value. The ENSO-related Indo-Pacific tropical sea surface temperature (SST) anomalies have been considered as the dominant externally-driven forcing of monsoon variability (Webster et al., 1998; Kumar et al., 2006). The dynamical linkage between these two systems principally results from the SST-induced east-west shifts in the Walker Circulation and its interaction with the regional monsoon Hadley circulation (Webster et al., 1998; Krishnamurthy and Goswami, 2000; Ashok et al., 2004). For example, El Niño's impact on ISM rainfall is particularly strong when the locus of deep atmospheric convection shifts to the central Pacific (Central El Niño) and the strongest descending lobe of the Walker cell is focused over the eastern equatorial Indian Ocean (Fasullo and Webster, 2002; Kumar et al., 1999, 2006) – driving an anomalous monsoon Hadley circulation whose descending limb suppresses the convection-driven monsoon rainfall over the Indian sub-continent. The extreme manifestation of this coupling is exemplified (albeit, sporadically) by the co-occurrence of large El Niño events and devastating droughts in the Indian sub-continent such as during 1876–1878, 1918–1919, and 1982–1983 (Kumar et al., 2006).

In observational data, the strength of the ENSO-Monsoon relationship (characterized by linear correlation between any of the broad indices of ISM rainfall and SST anomalies in the tropical Pacific, respectively) has varied on inter-decadal to multi-decadal timescales exhibiting high (low) inverse-correlation at times when the ENSO variance shows high (low) amplitude modulation (Torrence and Webster, 1999; Krishnamurthy and Goswami, 2000). This has led to the suggestion that ENSO effects ISM rainfall through the same physical mechanism on both interannual and interdecadal timescales and that the waxing and waning of the coupling is related to frequency/amplitude modulation of ENSO events and changes in the tropical Pacific

CPD
9, 3103–3123, 2013

mean state (Ummenhofer et al., 2011). The recent breakdown in the relationship between the two systems (e.g. Kumar et al., 1999) has however, occurred in the context of increased ENSO variance since the 1980's, with the late 20th century ENSO variability reaching a level as high as any other period during the last millennium (Li et al., 2011; Cobb et al., 2003, 2013). A range of hypotheses have been offered to explain the recent breakdown including global warming (Kumar et al., 1999), a southeastward shift of the subsiding limb of the Walker cell (Collins et al., 2010), changes in the ENSO spatial characteristics (Kumar et al., 2006), and the co-occurrence of ENSO and Indian Ocean Dipole (IOD) events (Ashok et al., 2004; Ummenhofer et al., 2011). In contrast, it has been argued that the relationship has largely remained intact and any fluctuations in its strength are merely a sampling artifact (Gershunov et al., 2001) such that low frequency changes in the correlation statistics between ENSO and the ISM timeseries' occurs much in the manner expected from purely stochastic processes.

Understanding the dynamical nature of the ENSO-Monsoon relationship using state-of-the-art general circulation models has been hampered by systematic errors in simulating the mean state and variability of both ENSO and the ISM systems (Annamalai et al., 2007; Collins et al., 2010). It is thus clear that empirical observations and model simulations alone are inadequate in assessing the long-term nature of the influence that ENSO has on the ISM which, as a consequence, limits the predictability of the monsoon system across timescales. Proxy reconstructions of ENSO and ISM can therefore provide much needed constraints on the nature of this coupling, particularly in the low frequency domain under varying climate boundary conditions. Here we utilize two continuous, well-dated, millennial-length reconstructions of the systems to shed light on the role ENSO plays in driving the multidecadal power that characterizes ISM variability over the last millennium (Berkelhammer et al., 2010).

CPD
9, 3103–3123, 2013

2 Methods

2.1 Monsoon reconstruction

A number of previous studies (e.g. Berkelhammer et al. (2010); Sinha et al. (2007, 2011) have demonstrated that ISM variability can be robustly reconstructed on a variety of timescales using the isotopic variability (δ^{18}O) of speleothems from central India. Here we utilize a continuous 1400 yr long ISM reconstruction derived from a pair of overlapping speleothems from two sites, Dandak and Jhumar Caves, located at ~ 19° N, 82° E in the southern region of the core monsoon zone (CMZ) defined here as ~ 18°–27° N and 69°–88° E (Fig. 1). Details on the sampling methodologies and age models of these two records are described in previous studies (Berkelhammer et al., 2010; Sinha et al., 2011) and for the purpose of this study we have taken the two published records (available here: http://www.ncdc.noaa.gov/paleo/speleothem.html), linearly interpolated them to an annual timescale and averaged the two (over the period of overlap) to produce a composite δ^{18}O record. We deem this compositing valid as the δ^{18}O profiles from Jhumar (2007–1075 AD) and Dandak (1562–625 AD) are well correlated (over the period of overlap) at $r = 0.62$ ($n = 353$; 95 % [0.43; 0.74]) suggesting the independent age models are valid and the isotopic variability is not a function of the local cave environment.

There is a significant (inverse) correlation between the speleothem δ^{18}O and CMZ JJAS precipitation (defined as the average of instrumental JJAS precipitation from 18° to 27° N and 69° to 88° E) timeseries' during the instrumental period (1903–2006 AD, $n = 70$, $r = -0.46$ with 95 % CI [−0.59; −0.32]) (Fig. 1). Significance and confidence intervals for the correlation estimates were obtained using block bootstrap resampling (Mudelsee, 2010), which takes into account deviations from normal distributional shape and temporal autocorrelation. Further validations of the technique comes from the observation that the record captures a number of known historical droughts such as those during 1876–1878 AD, 1861–1863 AD, and 1790–1796 AD (Sinha et al., 2007) and

CPD
9, 3103–3123, 2013

captures the series of protracted regional monsoon "megadroughts" in the late 14th century observed in tree ring records from SE Asia (Buckley et al., 2010).

The robustness of the speleothems in capturing monsoon variability arises from the presence of a strong "amount effect" (Dansgaard, 1964) over India, which has been documented in both modeling and observational studies (Dayem et al., 2010; Vuille et al., 2005; Pausata et al., 2011). In order to test the regional manifestation of the "amount effect" (i.e. its persistence and strength), we utilize simulations with a nudged Isotope-enabled GCM (Yoshimura et al., 2008), which has been validated for the ISM in a previous study (Berkelhammer et al., 2012). The model shows that the region from where this proxy was generated experiences a strong inverse relationship between the $\delta^{18}O$ in the precipitation ($\delta^{18}O_p$) and the modeled area-weighted precipitation amount over the CMZ (Fig. 2). Similar (or even more significant) correlation coefficients are also found for other broad ISM rainfall indices in the isotope simulations such as the Homogenous Monsoon Zone and the Indian Monsoon Index (IMI) (Wang and Fan, 1999; Wang et al., 2009), indicating the isotopic ratio in the precipitation at this site is a broad indicator of monsoon strength and not sensitive to domain boundaries or the choice of index.

The sensitivity of the isotopes in the precipitation, and consequently the proxy, to the overall strength of the Indian Monsoon system arises because of its location at the near distal end of the landward portion of the low level Jet that is the primary conduit for moisture transport from the Arabian Sea onto the Indian subcontinent (Fig. 2). As a consequence, the isotopic ratio in the vapor and the precipitation at this site aggregate all upstream processes (e.g. rainout) that have influenced the Arabian Sea branch of the monsoon system as it crosses the continent (Fig. 2). For example, mean westerly flow is weaker with a large reduction in moisture flux during anomalous monsoon seasons associated with El Niño events (Fasullo and Webster, 2002). The low level jet generates strong cyclonic vorticity in the boundary layer that aids in the initiation of convection over the entire CMZ region. The convective-related monsoon rainfall variability in the CMZ is significantly correlated (r = 0.75, 1901–2010 AD) to variations in

CPD
9, 3103–3123, 2013

the IMI (Wang et al., 2009; Goswami, 1998) region -broadly reflecting the large-scale rainfall variability in the region west of ∼80° E) on intraseasonal (e.g. Active and Break Periods) to inter-annual (e.g. ENSO events) timescales. While the upstream processes that influence the isotopic ratio in the moisture are myriad, and therefore a direct transfer between rainfall amount and $\delta^{18}O_p$ is not likely stationary or linear, these collective monsoonal processes are the dominant control on the annually-averaged $\delta^{18}O_p$ variability, explaining ∼25–30 % of the total variance of $\delta^{18}O$ in the speleothems.

2.2 ENSO reconstruction

A number of attempts have been made to reconstruct continuous centennial to millennial length timeseries of ENSO variability by extracting inter-annually resolved climate signals from tree rings and corals (Emile-Geay et al., 2013; Li et al., 2011; Cobb et al., 2013; Mann et al., 2009). These reconstructions are generally well-calibrated and verified though as a consequence of differences in the targeted index of ENSO to reconstruct, some significant differences can be found between the proxy records (Emile-Geay et al., 2013; Li et al., 2011). While the most accurate reconstructions of ENSO variability are presumably from proxies that are located within ENSO's center of action (i.e. the central tropical Pacific), such reconstructions are generally short and discontinuous. Proxy reconstructions from ENSO's teleconnected regions (such as the western United States) tend to be longer and continuous but rely on an assumption that the sign and strength of the teleconnection with ENSO has remained constant over time. Various ensembles of both direct and distal proxy reconstructions of ENSO show similar behavior at decadal to multidecadal scales but the amplitude of centennial variability, diverges between some proxies as a result of the choice of target SST dataset for calibration purpose (Emile-Geay et al., 2013).

We have chosen to utilize both a remote ENSO-teleconnection based proxy (Li et al., 2011) and a continuous section of the sporadic coral-based ENSO reconstruction of Cobb et al. (2003). The former is a millennial-length, continuous reconstruction of the

CPD
9, 3103–3123, 2013

canonical (eastern Pacific) ENSO amplitude derived from the gridded North American Drought Atlas (NADA) – a large dataset of tree ring based drought reconstructions (Cook et al., 2004). The variance of the first principal component (PC-1) of NADA is significantly correlated to various modern indices of ENSO based on the influence that ENSO has on moisture availability in the western North America. The record has excellent skill during the calibration period and agrees with shorter-term proxy reconstructions of ENSO including those derived from discontinuous coral sequences from the tropical Pacific and is currently the longest continuous ENSO reconstruction spanning the last millennium. We also utilize a reasonably long coral $\delta^{18}O$ sequence (spanning 1320–1460 AD) from Palmyra Island in the central tropical Pacific to validate our findings using an alternative to the remote-reconstruction.

2.3 Phase estimation

In order to assess the ISM-ENSO teleconnection, we look at coherence and phase angle between the two systems following a similar assessment of the modern ENSO-ISM teleconnection from Torrence and Webster (1999). Phase between the overlapping period of the ENSO reconstruction of Li et al. (2011) and the monsoon proxy (Sinha et al., 2011) is done using the multi-taper method (Chave et al., 1987). We focus discussion hereafter on two windows of the spectra, a *high frequency* band that includes all power in the 5–15 yr window and a *low frequency* band encompassing power in the 60–80 yr window. The high frequency band is intended to explore the long-term stability of the known dynamical connection between the monsoon and ENSO during the instrumental period. The high frequency band should assess variations at the interannual timescale however, as a consequence of multi-year mixing times for water in the karst, the monsoon proxy likely integrates variability across ~3–8 yr. Therefore we deem the 5–15 yr band as the highest frequency window in which confidence in the proxy can be asserted. The low frequency window was chosen as a response to earlier work based on one of the speleothems in the composite (i.e. Berkelhammer et al., 2010), which showed the presence of strong multidecadal power of the monsoon. The source of

CPD
9, 3103–3123, 2013

this multidecadal variability remains unknown as its period is too long to be studied using instrumental observations alone. The phase analysis presented here is therefore specifically intended to assess the role ENSO may play in pacing the dominant multidecadal power of the ISM.

To evaluate whether the differences in the phase angle between ENSO and the ISM in the low (≥ 60 yr) and high (≤ 15 yr) frequency bands are significant against the age-model uncertainties, we performed a numerical simulation where the timescale of two sinusoidal signals (frequencies *f1* and *f2* with predefined phase differences of d_{phi}) was "jittered" with a random number generator. We then estimated the phase difference for the jittered series, $d_{\text{phi}_{\text{sim}}}$ using a periodogram. The standard deviation of $d_{\text{phi}_{\text{sim}}}$ for the low-frequency bound $f1 = 1/(60\,\text{yr})$ and the high-frequency bound $f2 = 1/(15\,\text{yr.})$ was calculated from 10 000 simulations.

3 Results

A comparison between NADA PC-1 variance and the composite ISM speleothem $\delta^{18}O$ timeseries suggests that during most portions of the last millennium, multidecadal-length periods of enhanced (reduced) ENSO variance were associated with higher (lower) ISM rainfall (Fig. 3). The strength of this correlation is particularly strong between 900 and 1500 AD though continues, albeit intermittently, after the 15th century. For example, some of the wettest intervals of the ISM occur after the 17th century coinciding with a multi-centennial period of the highest ENSO variance in the NADA PC-1 reconstruction.

The cross spectra and phase coherence between the two timeseries, using the method described above, show the two timeseries' contain significant shared power in both the low (60–90 yr) and high (5–15 yr) frequency bands (Figs. 3 and 4). However, the angle of the phasing is nearly opposite in these two regions of the spectra such that in the high frequency band, enhanced ENSO variance occurs during periods of weakened monsoon (consistent with modern observations) and in the low frequency

CPD
9, 3103–3123, 2013

band enhanced ENSO variance is associate with a strengthened monsoon. Results from the 10 000 iteration Monte Carlo simulation illustrate that even with conservative estimates of age model uncertainty, the difference in the phase angle between ENSO and the ISM timeseries' in the high and low frequency windows are significant. We estimate uncertainty in the phase angle estimates could be as much as 52° while the phase angle difference we calculate is between 90 to 150°, attesting to the robustness of this finding (Fig. 3).

4 Discussion

The phase relationship between ENSO and the ISM in the multidecadal window suggests the nature of the coupling between these systems is contradictory to the relationship observed during the instrumental period where weak monsoons occur with positive ENSO events. To test the robustness of this finding against an alternative ENSO proxy, we compare portions of the ISM timeseries to a pair of coral sequences from Palmyra Island in the central tropical Pacific (Cobb et al., 2003) (Fig. 5). The continuous coral section that spans the late 14th and early 15th centuries fortuitously covers a critical portion of the ISM timeseries when the δ^{18}O values are among the highest of the last 1400 yr. As noted by Buckley et al. (2010) and Sinha et al. (2007), this period marks a protracted interval of weak monsoon. When speleothem and coral proxy records are scaled against their 20th century instrumentally-calibrated means, the coral-derived ENSO variance in the 2–7 yr band and speleothem-derived estimates of CMZ rainfall during the mid-14th century are significantly lower than the mean 20th century values (Fig. 5). While this comparison does not provide continuity, it does yield an independent assessment that ENSO and the ISM exhibit a counter-intuitive relationship in the multidecadal window.

The results of the phase analysis suggest that in the low-frequency domain, ENSO produces no consistent measurable impact on Indian Monsoon rainfall. There are indeed periods, such as the 20th century, when low frequency changes in ENSO

CPD
9, 3103–3123, 2013

variance appear to track the ISM in a dynamically sensibly way, however, in the context of the last 1000 yr these periods are rare (Fig. 3). The two systems do exhibit strong coherence in the 60–80 yr band such that the multidecadal power of the two systems may be phase-locked through a common forcing mechanism but because the phase angle is orthogonal to our expectations, the shared power cannot be through a direct causal relationship. One mechanism to explain the presence of shared power in this band is through the North Atlantic. It is well-documented that N. Atlantic SSTs yield power in the 60–80 yr range (Enfield et al., 2001) and impact both ENSO variance and the ISM. For example, Dong et al. (2006) document the presence of an atmospheric bridge where cooling in the North Atlantic yields an increase in ENSO variance. Goswami et al. (2006) show how cooling in the North Atlantic leads to an enhancement of the ISM through its influence on upper tropospheric temperatures. Therefore, a plausible explanation of the observations is that multidecadal shifts in the N. Atlantic SSTs exert an influence on both ENSO variance and the ISM and ultimately could phase lock the systems in a non-causal way.

An alternative, though not mutually exclusive, explanation of the results hinges on a reconsideration of the tree-ring ENSO proxy itself. For example, multidecadal variability in the North Atlantic influences water availability in the western US (McCabe et al., 2004) and therefore growth in water-limited trees (Conroy et al., 2009; Gray et al., 2003). Thus, variance in the PC-1 of NADA may also contain some power associated with the North Atlantic despite efforts to isolate only the ENSO signal (Li et al., 2011). In light of the phase relationship between ISM and NADA PC-1, it is therefore reasonable to suggest that the 60–80 yr power in the tree-ring derived ENSO reconstruction is a product of hydroclimatic shifts associated with multidecadal swings in the N. Atlantic (Sutton and Hodson, 2005). While it is beyond the scope of this work to distinguish whether the shared 60–80 yr power between NADA PC-1 record and the ISM is a function of the N. Atlantic's direct influence on western US hydroclimate or by way of its influence on ENSO variance, we ultimately arrive at the same conclusion, which is that

CPD
9, 3103–3123, 2013

the N. Atlantic is significantly more dominant than ENSO in pacing the ISM at these timescales.

A number of recent studies such as Tierney et al. (2013) argue for a dominant role for dynamics internal to the Indian Ocean (IO) in producing multidecadal hydroclimate variability across the IO Basin. IO dynamics are indeed a critical source of variance in the monsoon (Ashok et al., 2004) and likely an important determinant of low frequency monsoon behavior. However, if IO was pacing the multidecadal power in the monsoon, it is not clear why tree ring growth in the western US would be in phase with the ISM as we observe from our spectral analysis (Fig. 3). Therefore, in the absence of an established mechanism for IO dynamics to pace the hydroclimate of the western US, we are inclined to reject this mechanism.

5 Conclusions

Over the last millennium, the ISM has exhibited persistent multidecadal power. The protracted multidecadal shifts in precipitation amounts are significant in considering both flooding and drought frequency in India. The susceptibility of agricultural production to these hydroclimatic changes may be enhanced in coming decades as regional groundwater resources have been severely depleted and therefore may not be able to provide a buffer (Rodell et al., 2009). Through analysis of the phase relationship between proxies for ENSO and the ISM, we conclude that ENSO cannot be called upon to be the dominant driver of this multidecadal power despite its known role in producing strong monsoon drought in isolated years. The fact that ENSO and ISM proxies are in phase with one another at the multidecadal timescales provides an important constraint on the forcing mechanism pacing the ISM. Based on the teleconnection patterns associated with multidecadal N. Atlantic SST variability (i.e. its influence on the ISM, ENSO variance and W. US hydroclimate) and that its power is focussed between 60–90 yr, it seems an increasingly likely candidate to explain the proxy-reconstructed variance in the ISM. While the role of other forcing mechanisms in controlling the monsoon, such

CPD
9, 3103–3123, 2013

as the Indian Ocean should not be diminished, the linkage between the western US hydroclimate and ISM attest to the N. Atlantic as the multidecadal pacemaker of the ISM.

Acknowledgements. We gratefully acknowledge the National Science Foundation grant to A. S. (ATM: 0823554) and Chinese National Science Foundation support to H. C. for funding this research.

References

Annamalai, H., Hamilton, K., and Sperber, K.: The South Asian summer monsoon and its relationship with ENSO in the IPCC AR4 simulations, J. Climate, 20, 1071–1092, 2007. 3106

Ashok, K., Guan, Z., Saji, N., and Yamagata, T.: Individual and combined influences of ENSO and the Indian Ocean dipole on the Indian summer monsoon, J. Climate, 17, 3141–3155, 2004. 3105, 3106, 3114

Berkelhammer, M., Sinha, A., Mudelsee, M., Cheng, H., Edwards, R. L., and Cannariato, K.: Persistent multidecadal power of the Indian Summer Monsoon, Earth Planet. Sci. Lett., 290, 166–172, 2010. 3106, 3107, 3110, 3119

Berkelhammer, M., Sinha, A., Stott, L., Cheng, H., Pausata, F., and Yoshimura, K.: An abrupt shift in the Indian monsoon 4000 years ago, Geophys. Monogr. Ser., 198, 75–87, 2012. 3108

Buckley, B. M., Anchukaitis, K. J., Penny, D., Fletcher, R., Cook, E. R., Sano, M., Nam, L. C., Wichienkeeo, A., Minh, T. T., and Hong, T. M.: Climate as a contributing factor in the demise of Angkor, Cambodia, Proc. Natl. Acad. Sci. USA, 107, 6748–6752, doi:10.1073/pnas.0910827107, 2010. 3108, 3112

Chave, A. D., Thomson, D. J., and Ander, M. E.: On the robust estimation of power spectra, coherences, and transfer functions, J. Geophys. Res., 92, 633–648, doi:10.1029/JB092iB01p00633, 1987. 3110

Cobb, K. M., Charles, C. D., Cheng, H., and Edwards, R. L.: El Niño/Southern Oscillation and tropical Pacific climate during the last millennium, Nature, 424, 271–276, 2003. 3106, 3109, 3112, 3123

Cobb, K. M., Westphal, N., Sayani, H. R., Watson, J. T., Di Lorenzo, E., Cheng, H., Edwards, R., and Charles, C. D.: Highly Variable El Niño–Southern Oscillation Throughout the Holocene, Science, 339, 67–70, 2013. 3106, 3109

Collins, M., An, S.-I., Cai, W., Ganachaud, A., Guilyardi, E., Jin, F.-F., Jochum, M., Lengaigne, M., Power, S., Timmermann, A., Vecchi, G., and Wittenberg, A.: The impact of global warming on the tropical Pacific Ocean and El Niño, Nat. Geosci., 3, 391–397, 2010. 3106

Conroy, J. L., Overpeck, J. T., Cole, J. E., and Steinitz-Kannan, M.: Variable oceanic influences on western North American drought over the last 1200 years, Geophys. Res. Lett., 36, L17703, doi:10.1029/2009GL039558, 2009. 3113

Cook, E. R., Woodhouse, C. A., Eakin, C. M., Meko, D. M., and Stahle, D. W.: Long-term aridity changes in the western United States, Science, 306, 1015–1018, 2004. 3110

Dansgaard, W.: Stable isotopes in precipitation, Tellus, 16, 436–468, 1964. 3108

Dayem, K. E., Molnar, P., Battisti, D. S., and Roe, G. H.: Lessons learned from oxygen isotopes in modern precipitation applied to interpretation of speleothem records of paleoclimate from eastern Asia, Earth Planet. Sci. Lett., 295, 219–230, 2010. 3108

Dong, B., Sutton, R. T., and Scaife, A. A.: Multidecadal modulation of El Nino–Southern Oscillation (ENSO) variance by Atlantic Ocean sea surface temperatures, Geophys. Res. Lett., 33, L08705, doi:10.1029/2006GL025766, 2006. 3113

Draxler, R. and Rolph, G.: HYSPLIT (HYbrid Single-Particle Lagrangian Integrated Trajectory) model access via NOAA ARL READY website http://www.arl.noaa.gov/ready/hysplit4.html, NOAA Air Resources Laboratory, Silver Spring, 2003. 3120

Emile-Geay, J., Cobb, K. M., Mann, M. E., and Wittenberg, A. T.: Estimating Central Equatorial Pacific SST variability over the Past Millennium. Part 2: Reconstructions and Implications, J. Climate, 2013. 3109

Enfield, D. B., Mestas-Nuñez, A. M., and Trimble, P. J.: The Atlantic Multidecadal Oscillation and its relation to rainfall and river flows in the continental US, Geophys. Rese. Lett., 28, 2077–2080, 2001. 3113

Fasullo, J. and Webster, P.: Hydrological signatures relating the Asian summer monsoon and ENSO, J. Climate, 15, 3082–3095, 2002. 3105, 3108

Gershunov, A., Schneider, N., and Barnett, T.: Low-frequency modulation of the ENSO-Indian monsoon rainfall relationship: Signal or noise?, J. Climate, 14, 2486–2492, 2001. 3106

Goswami, B.: Interannual variations of Indian summer monsoon in a GCM: External conditions versus internal feedbacks, J. Climate, 11, 501–522, 1998. 3109

Goswami, B. N., Madhusoodanan, M., Neema, C., and Sengupta, D.: A physical mechanism for North Atlantic SST influence on the Indian summer monsoon, Geophys. Res. Lett., 33, L02706_1–L02706_4, doi:10.1029/2005GL024803, 2006. 3113

CPD
9, 3103–3123, 2013

Gray, S. T., Betancourt, J. L., Fastie, C. L., and Jackson, S. T.: Patterns and sources of multidecadal oscillations in drought-sensitive tree-ring records from the central and southern Rocky Mountains, Geophys. Res. Lett., 30, 1316, doi:10.1029/2002GL016154, 2003. 3113

Krishnamurthy, V. and Goswami, B. N.: Indian monsoon-ENSO relationship on interdecadal timescale, J. Climate, 13, 579–595, 2000. 3105

Kumar, K. K., Rajagopalan, B., and Cane, M. A.: On the weakening relationship between the Indian monsoon and ENSO, Science, 284, 2156–2159, 1999. 3105, 3106

Kumar, K. K., Rajagopalan, B., Hoerling, M., Bates, G., and Cane, M.: Unraveling the mystery of Indian monsoon failure during El Niño, Science, 314, 115–119, 2006. 3105, 3106

Li, J., Xie, S.-P., Cook, E. R., Huang, G., D'Arrigo, R., Liu, F., Ma, J., and Zheng, X.-T.: Interdecadal modulation of El Niño amplitude during the past millennium, Nat. Clim. Change, 1, 114–118, 2011. 3106, 3109, 3110, 3113, 3121

Mann, M. E., Zhang, Z., Rutherford, S., Bradley, R. S., Hughes, M. K., Shindell, D., Ammann, C., Faluvegi, G., and Ni, F.: Global signatures and dynamical origins of the Little Ice Age and Medieval Climate Anomaly, Science, 326, 1256–1260, 2009. 3109

McCabe, G. J., Palecki, M. A., and Betancourt, J. L.: Pacific and Atlantic Ocean influences on multidecadal drought frequency in the United States, Proc. Natl. Acad. Sci., 101, 4136–4141, 2004. 3113

Mudelsee, M.: Climate time series analysis: classical statistical and bootstrap methods, Vol. 42, Springer, 2010. 3107

Pausata, F. S., Battisti, D. S., Nisancioglu, K. H., and Bitz, C. M.: Chinese stalagmite [delta] 18O controlled by changes in the Indian monsoon during a simulated Heinrich event, Nat. Geosci., 4, 474–480, 2011. 3108

Rodell, M., Velicogna, I., and Famiglietti, J. S.: Satellite-based estimates of groundwater depletion in India, Nature, 460, 999–1002, 2009. 3114

Sinha, A., Cannariato, K. G., Stott, L. D., Cheng, H., Edwards, R. L., Yadava, M. G., Ramesh, R., and Singh, I. B.: A 900-year (600 to 1500 AD) record of the Indian summer monsoon precipitation from the core monsoon zone of India, Geophys. Res. Lett., 34, L16707, doi:10.1029/2007GL030431, 2007. 3107, 3112

Sinha, A., Berkelhammer, M., Stott, L., Mudelsee, M., Cheng, H., and Biswas, J.: The leading mode of Indian Summer Monsoon precipitation variability during the last millennium, Geophys. Res. Lett., 38, L15703, doi:10.1029/2011GL047713, 2011. 3107, 3110, 3119

CPD
9, 3103–3123, 2013

Sutton, R. T. and Hodson, D. L.: Atlantic Ocean forcing of North American and European summer climate, Science, 309, 115–118, 2005. 3113

Tierney, J. E., Smerdon, J. E., Anchukaitis, K. J., and Seager, R.: Multidecadal variability in East African hydroclimate controlled by the Indian Ocean, Nature, 493, 389–392, 2013. 3114

Torrence, C. and Webster, P. J.: Interdecadal changes in the ENSO-monsoon system, J. Climate, 12, 2679–2690, 1999. 3105, 3110

Ummenhofer, C. C., Gupta, A. S., Li, Y., Taschetto, A. S., and England, M. H.: Multi-decadal modulation of the El Nino–Indian monsoon relationship by Indian Ocean variability, Environ. Res. Lett., 6, 034006, doi:10.1088/1748-9326/6/3/034006, 2011. 3106

Vuille, M., Werner, M., Bradley, R., and Keimig, F.: Stable isotopes in precipitation in the Asian monsoon region, J. Geophys. Res., 110, D23108–1, doi:10.1029/2005JD006022, 2005. 3108

Wang, B. and Fan, Z.: Choice of South Asian summer monsoon indices, B. Am. Meteorol. Soc., 80, 629–638, 1999. 3108

Wang, B., Ding, Q., and Joseph, P.: Objective Definition of the Indian Summer Monsoon Onset, J. Climate, 22, 3303–3316, 2009. 3108, 3109

Webster, P. J., Maga a, V., Palmer, T., Shukla, J., Tomas, R., Yanai, M., and Yasunari, T.: Monsoons: Processes, predictability, and the prospects for prediction, J. Geophys. Res., 103, 14451–14510, doi:10.1029/97JC02719, 1998. 3105

Yoshimura, K., Kanamitsu, M., Noone, D., and Oki, T.: Historical isotope simulation using reanalysis atmospheric data, J. Geophys. Res., 113, D19108, doi:10.1029/2008JD010074, 2008. 3108, 3120

CPD
9, 3103–3123, 2013

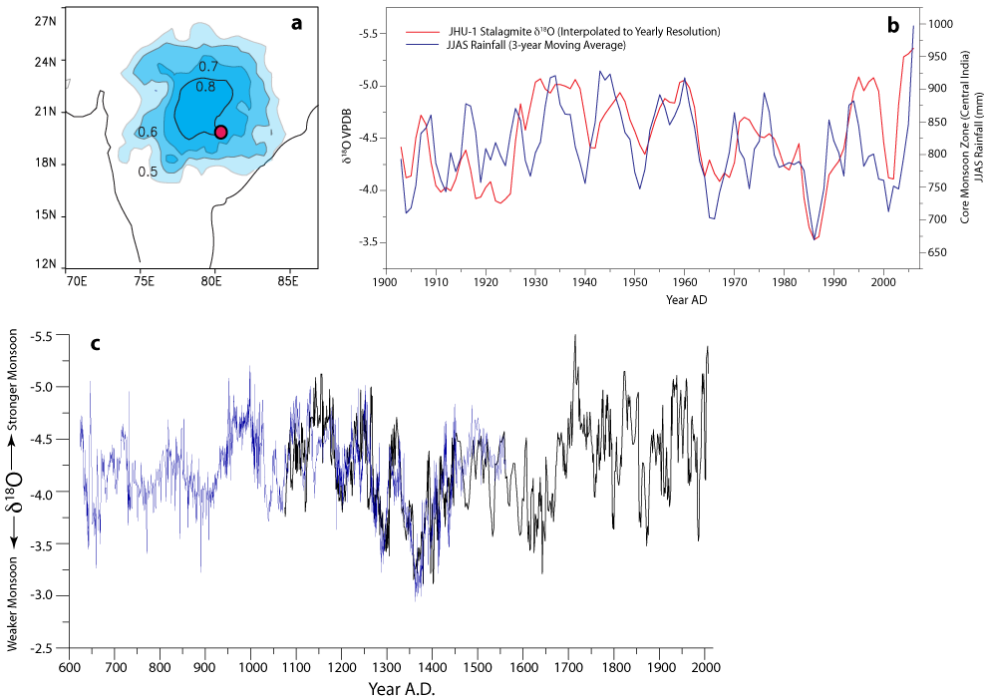

Fig. 1. (a) Correlation map between JJAS precipitation and regional precipitation across India. The result indicates the significance of this site as a broad indicator of CMZ monsoon precipitation. **(b)** The 20th century section of the speleothem δ^{18}O and JJAS rainfall from the nearest gauge. The observed precipitation amounts were treated with a 3 yr smooth to mimic mixing of waters in the karst. **(c)** The complete δ^{18}O timeseries from the JHU-1 (black) and Dandak (blue) records. Details of these records can be found in (Sinha et al., 2011) and (Berkelhammer et al., 2010).

CPD
9, 3103–3123, 2013

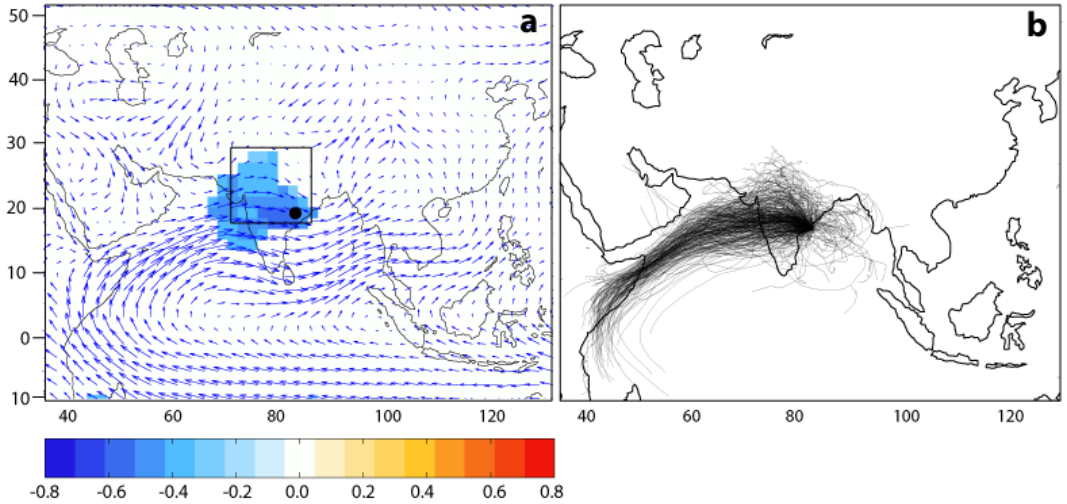

Fig. 2. (a) Correlation between JJAS $\delta^{18}O_p$ from nearest grid cell to the proxy and the precipitation rates in the surrounding grid cells using the IsoGSM model of Yoshimura et al. (2008). The analysis shows how upstream precipitation across India become aggregated in $\delta^{18}O_p$ at the proxy site. The vectors indicate the average surface wind fields during JJAS **(b)** A composite of 2400 trajectories from 2002–2011 using the Hysplit model (Draxler and Rolph, 2003). Each trajectory was run for 90 h from the proxy and initialized twice per day at 06:00 UTC and 12:00 UTC at 1500 m above ground level.

CPD
9, 3103–3123, 2013

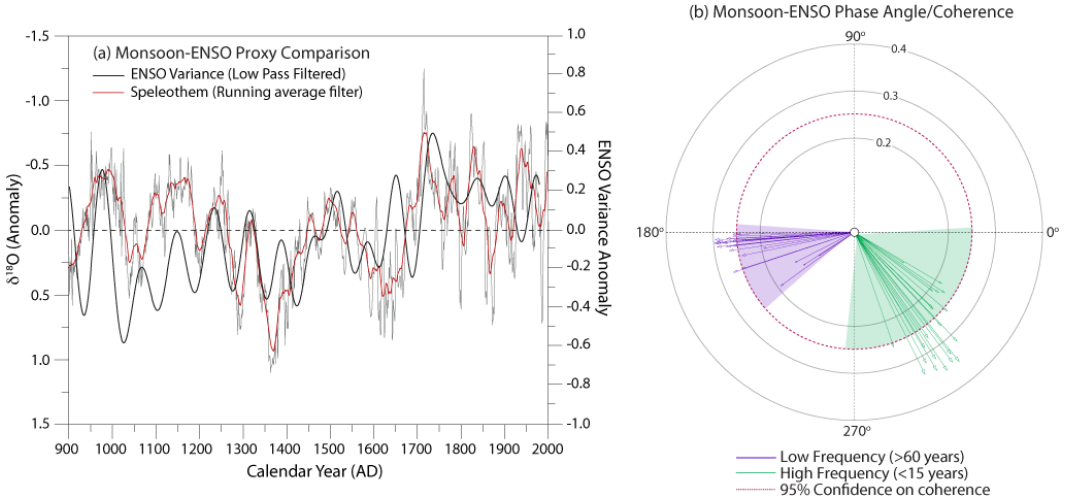

Fig. 3. (a) ISM proxy from Fig. 1 on an annually-interpolated timescale (red and gray) and the record of ENSO variance based on the PC-1 of the North American Drought Atlas from Li et al. (2011) (black). The ENSO timeseries was filtered to accentuate the multidecadal power in the timeseries. **(b)** Phase angle and coherence (length of arrows) between the two timeseries in the high (green) and low (purple) frequency windows as described in the text and shown in Fig. 4. Each individual arrow marks a 1° step in the spectra between 60–80° for purple and 5–15° for green. The length of the arrow indicates the strength of the phase coherence and the dotted line indicates where coherence is significant. Errors are estimated using a monte-carlo approach as described in the text. The clustering of purple arrows near 180° indicates the presence of anti-phased behavior in the low frequency domain between ENSO variance and ISM $\delta^{18}O$.

CPD
9, 3103–3123, 2013

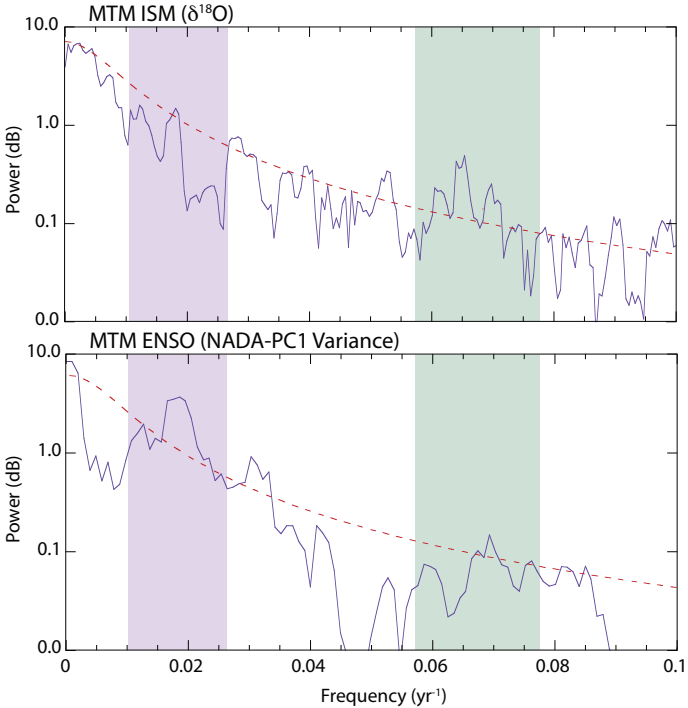

Fig. 4. Spectral analysis of the ISM and ENSO variance timeseries' using the Multi-taper method. Purple and green bands indicate the regions of the spectra (low and high frequency, respectively) used in Fig. 3 to assess the phase angle and coherence between the timeseries'. Red dotted line indicated the 95 % confidence interval using a Monte Carlo simulation.

CPD
9, 3103–3123, 2013

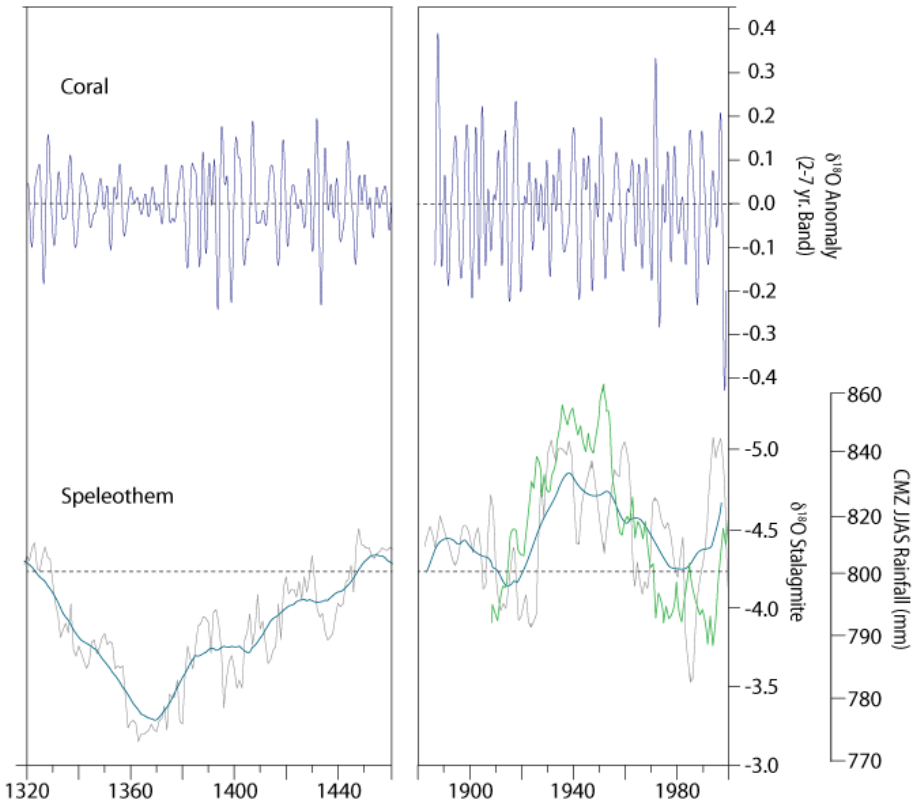

Fig. 5. A comparison between two coral sections from Cobb et al. (2003) (top) and the ISM proxy shown in Figs. 1 and 3. The coral record has been filtered to accentuate variance in the 2–7 yr band. The ISM is shown both raw (gray) and with a low pass filter (blue). The green line is the instrumental monsoon rainfall from the CMZ.

CPD
9, 3103–3123, 2013